Accepted for publication in The Astrophyical Journal

Globular clusters in the outer Galactic halo: new HST/ACS imaging of 6 globular clusters and the Galactic globular cluster age-metallicity relation [1]

Aaron Dotter

Space Telescope Science Institute, 3700 San Martin Dr., Baltimore, MD 21218

Ata Sarajedini

Department of Astronomy, University of Florida, 211 Bryant Space Science Center, Gainesville, FL 32611

Jay Anderson

Space Telescope Science Institute, 3700 San Martin Dr., Baltimore, MD 21218

ABSTRACT

Color-magnitude diagrams (CMDs) derived from Hubble Space Telescope (HST) Advanced Camera for Surveys $F606W, F814W$ photometry of 6 globular clusters (GCs) are presented. The six GCs form two loose groupings in Galactocentric distance (R_{GC}): IC 4499, NGC 6426, and Ruprecht 106 at ∼15-20 kpc and NGC 7006, Palomar 15, and Pyxis at ∼ 40 kpc. The CMDs allow the ages to be estimated from the main sequence turnoff in every case. In addition, the age of Palomar 5 ($R_{GC} \sim 18$ kpc) is estimated using archival HST Wide Field Planetary Camera 2 V, I photometry. The age analysis reveals the following: IC 4499, Ruprecht 106, and Pyxis are 1-2 Gyr younger than inner halo GCs with similar metallicities; NGC 7006 and Palomar 5 are marginally younger than their inner halo counterparts; NGC 6426 and Palomar 15, the two most metal-poor GCs in the sample, are coeval with all the other metal-poor GCs within the uncertainties. Combined with our previous efforts, the current sample provides strong evidence that the Galactic GC age-metallicity relation consists of two distinct branches. One suggests a rapid chemical enrichment in the inner Galaxy while the other suggests prolonged GC formation in the outer halo. The latter is consistent with the outer halo GCs forming in dwarf galaxies and later being accreted by the Milky Way.

Subject headings: globular clusters: general — Galaxy: formation

1. Introduction

The Galactic globular clusters (GCs) have long been recognized as useful probes of the formation and evolution of the Galaxy. Their spatial coherence allows their locations in age, metallicity, and Galactocentric distance (R_{GC}) space to be established with some accuracy. Their numbers allow them to be used as probes of the formation timescale and chemical enrichment history of the Milky Way halo, thick disk, and central bulge.

One of the earliest papers to examine the age-metallicity relation (AMR) of the Milky Way GC system was Sarajedini & King (1989). They calculated ages for 32 GCs using the magnitude difference between the horizontal branch (HB) and the main sequence turnoff (MSTO). Taking a cue from Gratton (1985), Sarajedini & King (1989) compared the AMR for GCs inside 15 kpc of the Galactic center with that of GCs outside 15 kpc. They found a statistically significant difference between the two: the AMR of GCs with Galactocentric distance (R_{GC}) < 15 kpc was shallower than that of GCs with $R_{GC} > 15$ kpc. Sarajedini & King (1989) argued, based on the work of Larson (1972) and Tinsley & Larson (1978), that the inner halo GCs formed in a region of higher gas and dust density, thereby accelerating GC formation and chemical enrichment. In contrast, the outer halo GCs formed in lower density sub-galactic fragments in a slower, more chaotic fashion akin to the fragmentation and accretion scenario advocated by Searle & Zinn (1978, see also Navarro et al. 1997) and featured in models of galaxy formation based on the cold dark matter paradigm with a cosmological constant (e.g., Zentner & Bullock 2003; Robertson et al. 2005; Font et al. 2006).

Subsequent work by Chaboyer et al. (1992), Sarajedini, Lee, & Lee (1995), and Chaboyer et al. (1996) reinforced the results of Gratton (1985) and Sarajedini & King (1989) using larger and more reliable data sets of GC ages as well as a variety of techniques for measuring them. The most recent studies to determine ages from a large sample of GCs, by Marín-Franch et al. (2009) and Dotter et al. (2010), rely upon the uniform photometric data set provided by the Hubble Space Telescope (HST) Advanced Camera for Surveys (ACS) Galactic GC Treasury project (Sarajedini et al. 2007). This data set provides deep photometry for 65 GCs of up to $\sim$7 magnitudes below the MSTO (Anderson et al. 2008). Based on a careful analysis of the

[1]Based on observations with the NASA/ESA *Hubble Space Telescope*, obtained at the Space Telescope Science Institute, which is operated by AURA, Inc., under NASA contract NAS 5-26555, under program GO-11586.

ages and metallicities of the Galactic GC Treasury project GCs, Marín-Franch et al. (2009) showed the clearest evidence thus far that the GC AMR splits into two distinct branches. This result was reinforced by Dotter et al. (2010), who added the six most distant (known) Galactic GCs to the GC Treasury data set and used the combined sample to study the correlations between HB morphology and a variety of GC parameters. The analysis presented by Forbes & Bridges (2010) using data assembled from the literature for 93 GCs largely reinforces these conclusions.

The HST/ACS Galactic GC Treasury project preferentially targeted nearby GCs in order to maximize the depth that could be achieved with one orbit per filter. One consequence of this strategy is that it left out much of the outer halo. The most distant GC observed as part of the Treasury project is NGC 4147 at $R_{GC} \sim 21$ kpc. Yet there are many GCs beyond this distance that can provide more leverage on the formation and subsequent evolution of the outer Galactic halo.

A number of investigators have used HST Wide Field Planetary Camera 2 (WFPC2) photometry to derive the ages of GCs with $R_{GC} > 50$ kpc. Harris et al. (1997) presented deep photometry of NGC 2419 ($R_{GC} \sim 90$ kpc; Harris 1996, 2010 revision) and concluded that it is coeval with the similarly metal-poor GC M 92 based on a differential comparison of their color-magnitude diagrams (CMDs). Stetson et al. (1999) obtained deep photometry of Palomar 3, Palomar 4, and Eridanus (all with $R_{GC} > 90$ kpc) and concluded that the three are ∼1.5-2 Gyr younger than the relatively nearby GCs M 3 and M 5. Their conclusion rests on the assumption that the outer halo GCs have similar chemical abundances ([Fe/H] and [α/Fe]) to M 3 and M 5; this assumption has since been borne out for Palomar 3 (Koch et al. 2009) and Palomar 4 (Koch & Côté 2010). Dotter et al. (2008) presented CMDs of Palomar 14 ($R_{GC} \sim 75$ kpc) and AM-1 ($R_{GC} \sim 125$ kpc) and concluded that both are 1.5-2 Gyr younger than M 3, in keeping with the results of Stetson et al. (1999). For the purposes of the present study, the 6 known GCs with $R_{GC} > 50$ kpc are sufficiently well studied to firmly mark their place in the GC AMR. Chemical abundance information remains rather sparse for the most distant GCs, but what is known is consistent with what has been inferred from the CMDs.

Thus far then, deep and fairly homogeneous HST CMDs in the V and I (or equivalent) filters exist for the majority of GCs with $R_{GC} \lesssim 15$ kpc and all those (known) beyond 50 kpc, allowing precise and internally consistent ages to be measured. What remains is to target the GCs within $15 \lesssim R_{GC} \lesssim 50$ kpc so that the complete radial extent of the Galactic GCs, and what it can tell us about the formation of the Galaxy, can be probed. The present study is the first major step toward fulfilling this goal, wherein we present deep, homogeneous HST ACS photometry, and use the resulting CMDs to estimate the ages, of six outer halo GCs:

Pyxis, Ruprecht 106, IC 4499, NGC 6426, NGC 7006, and Palomar 15. Of the six, only IC 4499 has previous HST photometry (Piotto et al. 2002), and it is not of sufficient depth to allow an accurate age determination. In addition, a new age determination for Palomar 5 ($R_{GC} \sim 18$ kpc) using archival HST/WFPC2 V, I data from Grillmair & Smith (2001) has been performed and included in the subsequent discussion.

The remainder of this paper proceeds as follows: the observations and data reduction are described in §2, the CMDs are presented in §3, the available information on the chemical abundances, distances, and reddening values of the sample is reviewed in §4, new age determinations based on isochrone fitting are presented in §5, the Galactic GC AMR is updated and compared with theoretical work in the context of the formation of the Galaxy in §6, §7 provides some discussion of the results, and §8 summarizes the findings presented in the paper.

2. Observations and Data Reduction

The observations were obtained with the HST/ACS Wide Field Channel (WFC) under program number GO-11586 (PI: Dotter) during Cycle 17. Table 1 shows the observing log. The ACS images were retrieved from the HST archive and calibrated using the pipeline bias and flat-field procedures. All clusters, except for Palomar 15, were imaged over two orbits with the first orbit devoted to $F606W$ and the second to $F814W$. Palomar 15 is the most distant and reddened in the sample and it received a total of five orbits: two in $F606W$ and three in $F814W$.

Photometry and astrometry were extracted from the images using the programs developed for GO-10775, the ACS Survey of Galactic Globular Clusters, as described by Anderson et al. (2008). The observing strategy in the current program was designed to fol-

Table 1. GO-11586 Observations

Cluster	Data set	Date	RA	Dec	PA_V3	F606W	F814W
Pyxis	jb1601	11/10/2009	09h07m57.7s	-37:13:17.0	76.86	50s, 4 × 517s	55s, 4 × 557s
Ruprecht 106	jb1602	04/07/2010	12h38m40.1s	-51:09:00.9	287.34	55s, 4 × 550s	60s, 4 × 585s
IC 4499	jb1603	01/07/2010	15h00m18.5s	-82:12:49.5	235.97	60s, 4 × 603s	65s, 4 × 636s
NGC 6426	jb1604	04/08/2009	17h44m54.6s	+03:10:13.0	294.67	45s, 4 × 500s	50s, 4 × 540s
NGC 7006	jb1605	05/10/2009	21h01m29.4s	+16:11:14.4	275.03	45s, 4 × 505s	50s, 4 × 545s
Palomar 15	jb1606	16/10/2009	16h59m50.9s	-00:32:17.9	261.25	10s, 4 × 550s	10s, 4 × 500s
...						65s, 4 × 550s	25s, 4 × 560s
...							55s, 4 × 525s

low the identical pattern of exposure times and dithers as GO-10775. Since Anderson et al. (2008) give an extremely detailed description of the data reduction process, only those aspects that have changed in the interim will be mentioned here.

Before performing photometry on the individual images, they were corrected for charge transfer efficiency using the algorithm developed by Anderson & Bedin (2010). The instrumental photometry was then calibrated to the HST VEGAmag system following Bedin et al. (2005) and using the aperture corrections from Sirianni et al. (2005) as described by Sarajedini et al. (2007) and Anderson et al. (2008). The VEGAmag photometric zeropoints were obtained from Bohlin (2007). The photometric catalogs and supporting data files from the reduction process of the 6 GCs presented herein will be made publicly available through the same archive that will host the ACS GC Treasury database.

3. Color-Magnitude Diagrams

The $F606W, F606W - F814W$ CMDs are presented in Figures 1 through 6. Typical photometric errors are demonstrated towards the left side of each figure. In cases where ground-based V, I data are available, we also make a direct comparison with the ACS data converted to V and I using the empirical transformations provided by Sirianni et al. (2005). The ground-based comparisons indicate, in all cases, that the HST photometric system maintains a high degree of homogeneity post-SM4 and that the transformations to ground-based V and I magnitudes perform well.

The CMDs reveal several striking features. In particular, it can be seen that Ruprecht 106 and IC 4499 have strong binary and blue straggler sequences. NGC 6426, Palomar 15, and Pyxis show signs of differential reddening and, indeed, these are the most reddened clusters in the present sample. Palomar 15 and Pyxis are sparsely populated clusters; the red giant branch (RGB) of Pyxis loses coherence for $F606W \lesssim 19$.

4. Previous studies

This section provides a brief review of noteworthy studies targeting the GCs considered in the present study. A few basic parameters are collected in Table 2.

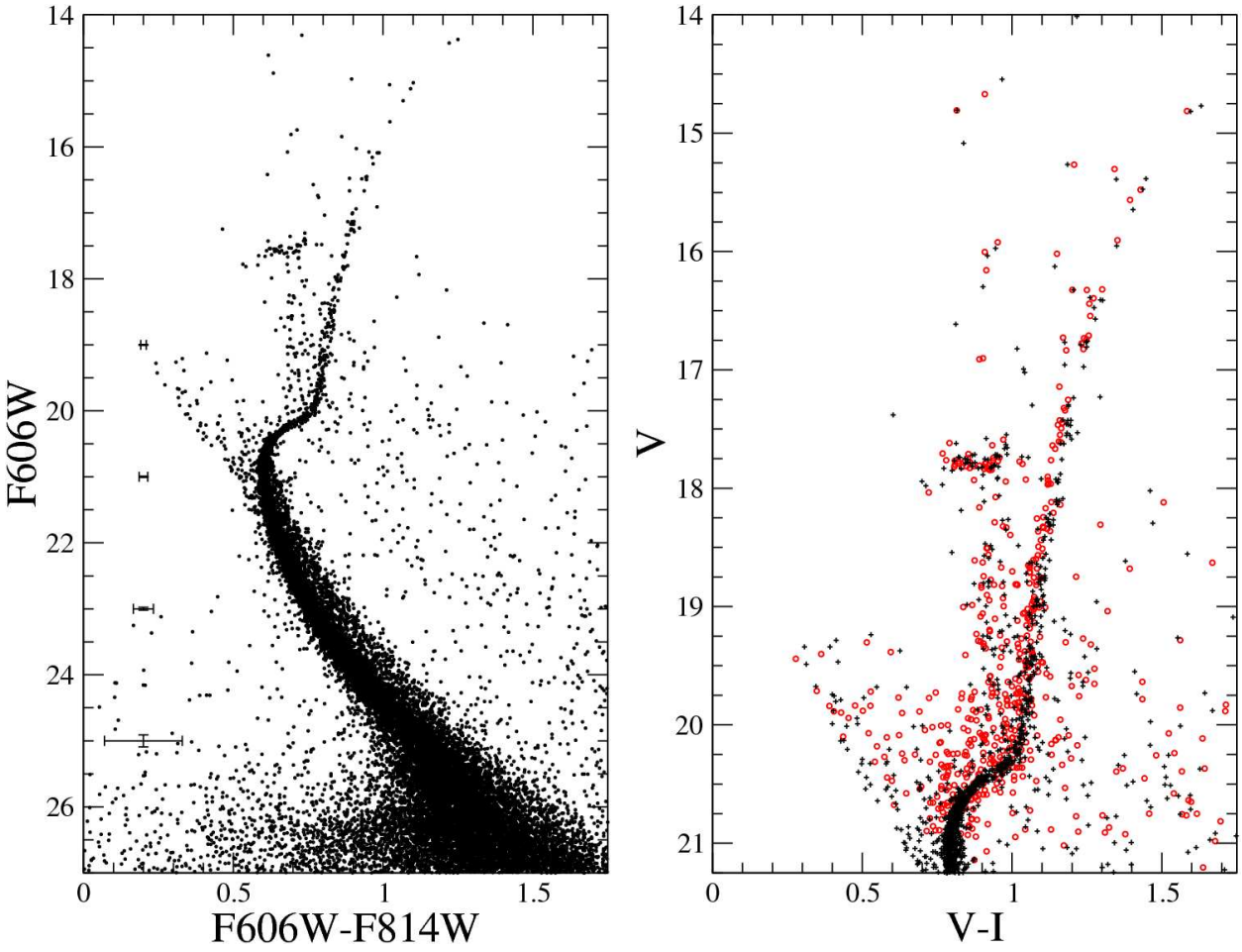

Fig. 1.— Left: The $F606W-F814W$ CMD of Ruprecht 106. Right: The ACS data (crosses), converted to V and I, compared with the ground-based V and I data of Sarajedini & Layden (1997, open circles).

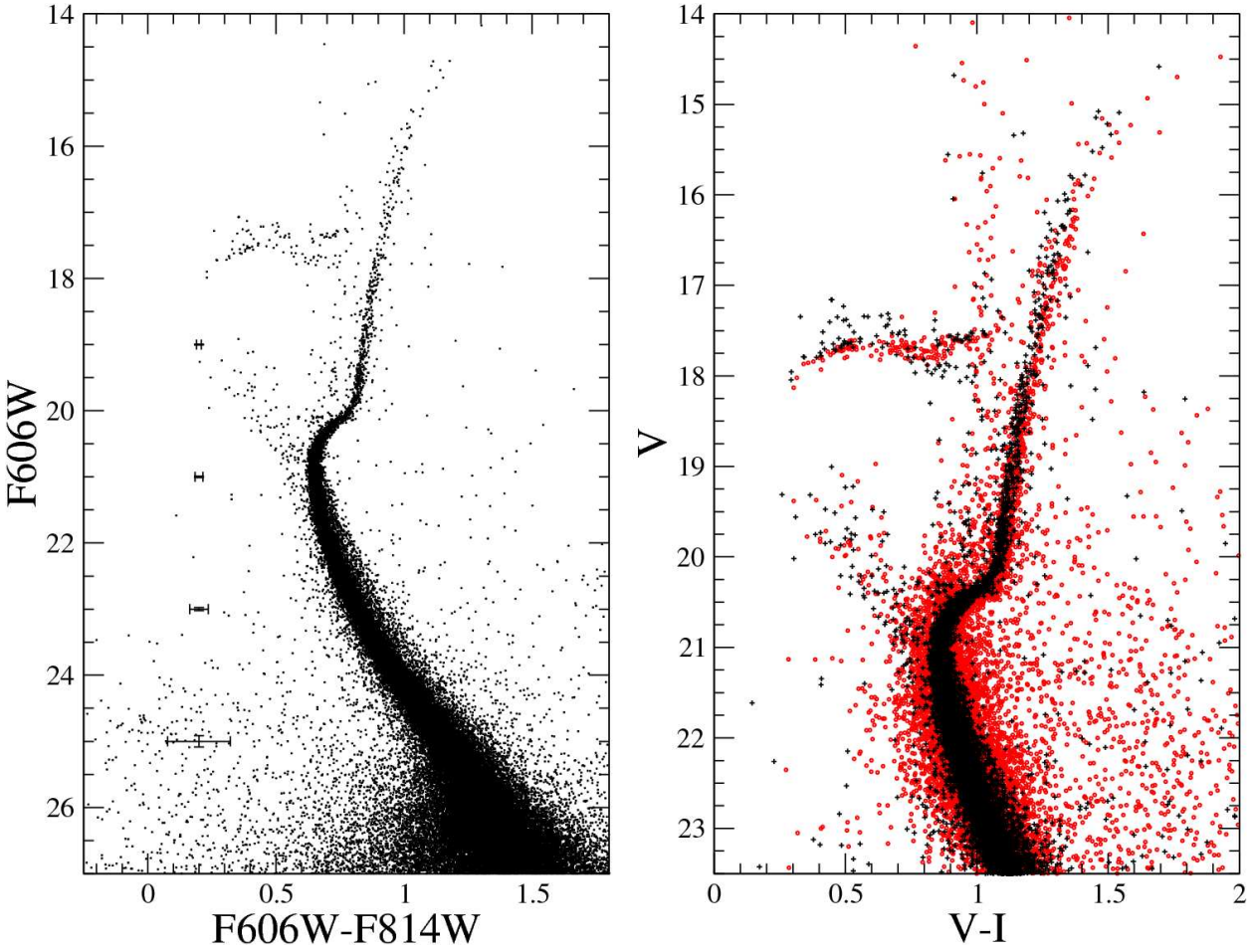

Fig. 2.— Left: The $F606W - F814W$ CMD of IC 4499. Right: The ACS data (crosses), converted to V and I, compared with the V, I data of Walker et al. (2011, open circles).

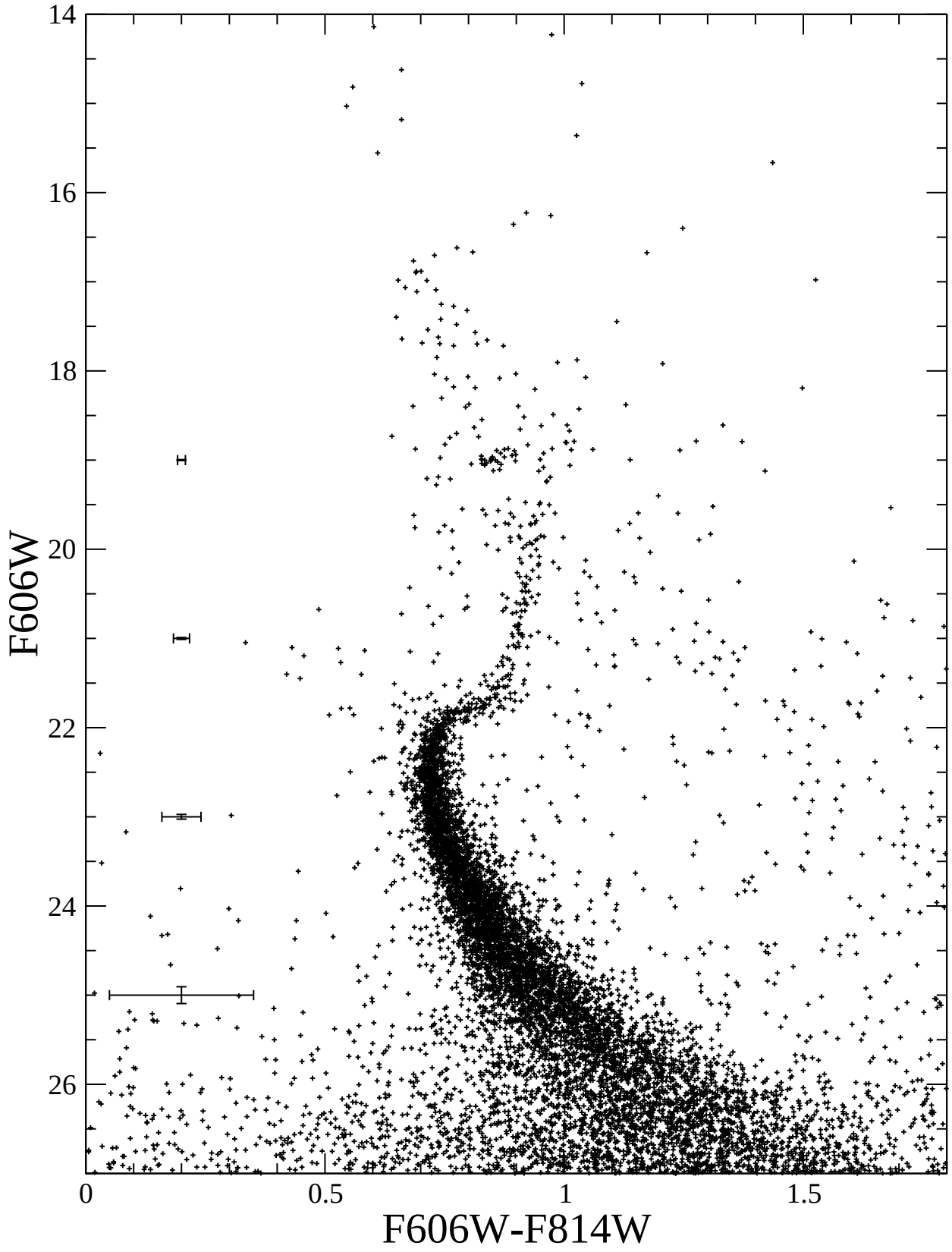

Fig. 3.— The $F606W - F814W$ CMD of Pyxis.

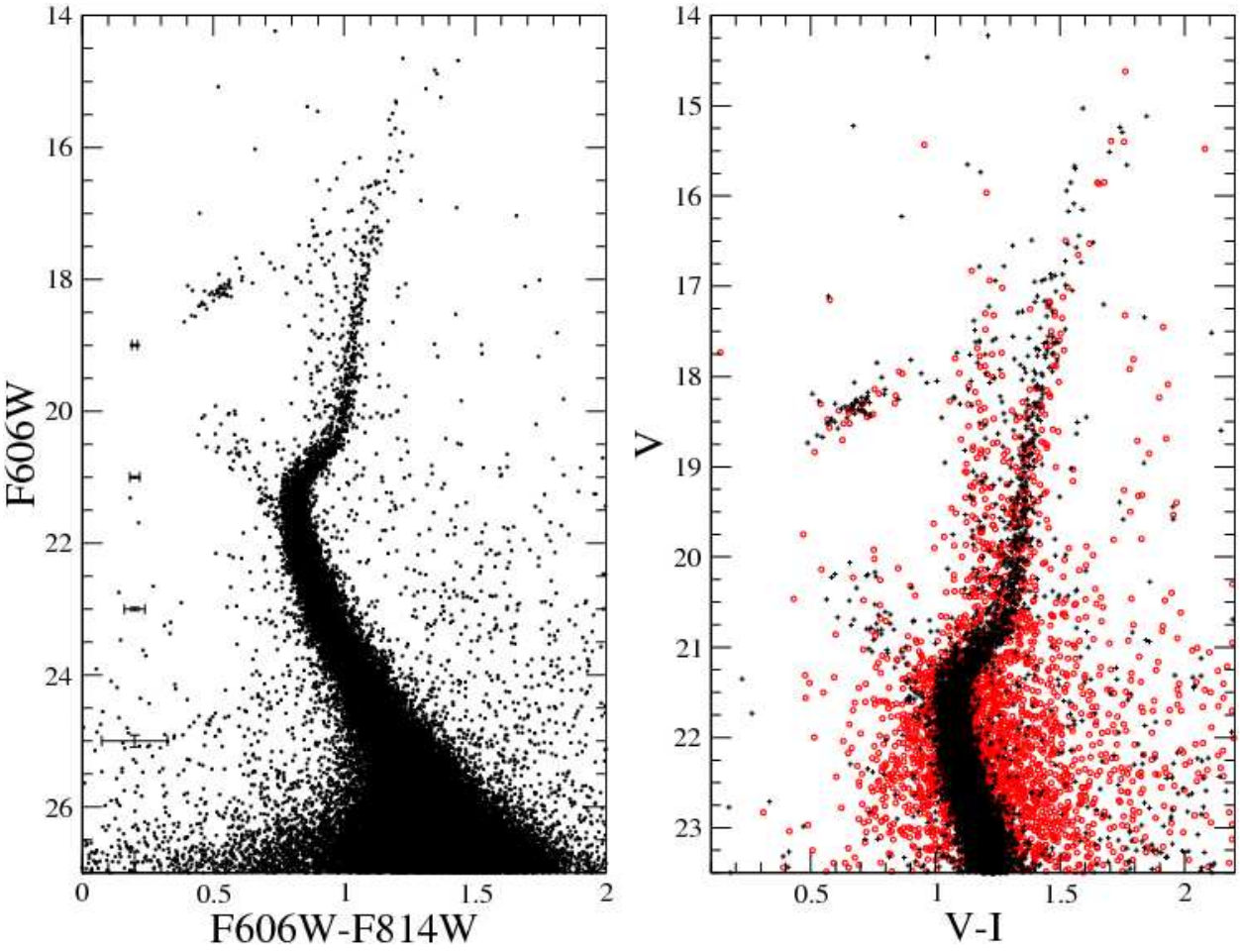

Fig. 4.— Left: The $F606W - F814W$ CMD of NGC 6426. Right: The ACS data (crosses), converted to V and I, compared with the V, I data of Hatzidimitriou et al. (1999, open circles).

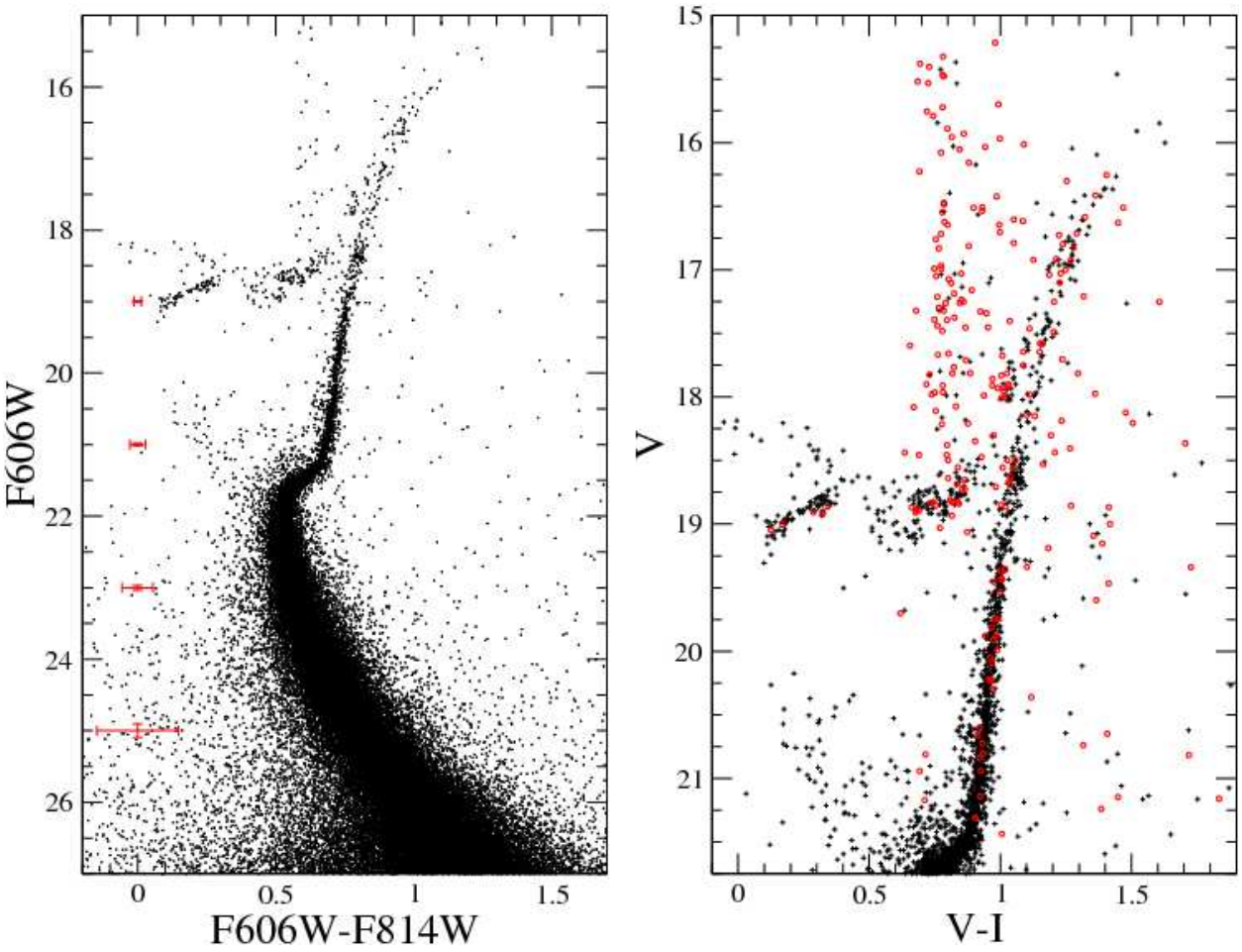

Fig. 5.— Left: The $F606W - F814W$ CMD of NGC 7006. Right: The ACS data (crosses), converted to V and I, compared with the V, I data of Stetson (2000, open circles).

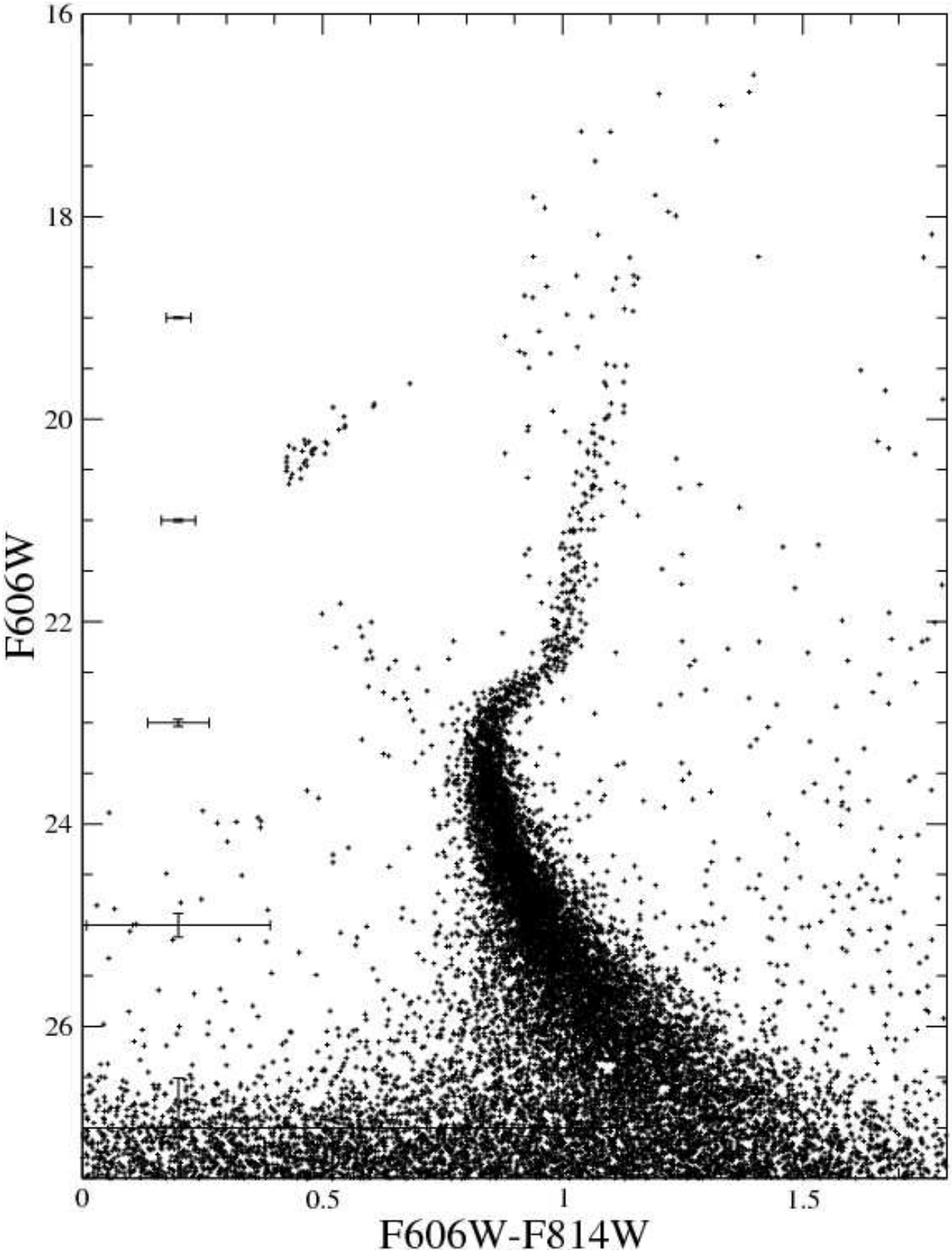

Fig. 6.— The $F606W - F814W$ CMD of Palomar 15.

Table 2. Literature values of basic cluster parameters

Cluster	DM_V (Harris)	$E(B-V)$ (Harris)	$E(B-V)$ (SFD98)	[Fe/H] (Harris)	[α/Fe]
IC 4499	17.09	0.23	0.224	-1.6	$\cdots$
Ruprecht 106	17.25	0.20	0.174	-1.5^a	$\sim 0.0^a$
NGC 6426	17.70	0.36	0.346	-2.26	$\cdots$
NGC 7006	18.24	0.05	0.082	-1.55^b	$+0.23^b$
Pyxis	18.65	0.21	0.327	-1.4^c	$\cdots$
Palomar 15	19.49	0.40	0.394	-2.0^d	$\cdots$
Palomar 5	16.92	0.03	0.056	-1.3^e	$+0.16^e$

References. — Sources of data are listed in the column headers except where otherwise specified. Harris–Harris (1996); SFD98–Schlegel et al. (1998); (*a*) P. Francois (2010) priv. comm.; (*b*) Kraft et al. (1998); (*c*) Palma et al. (2000); (*d*) Da Costa & Armandroff (1995); (*e*) Smith et al. (2002)

4.1. NGC 6426

The first modern CMD of this cluster was presented by Zinn & Barnes (1996) based on imaging with the 1-m telescope at Cerro Tololo Inter-American Observatory. Their CMD extended ∼3 mags below the HB and confirmed the identity of 12 variable stars in the cluster. Hatzidimitriou et al. (1999) and Papadakis et al. (2000) published $BVRI$ photometry extending to about 1 mag below the MSTO and an extensive study of its RR Lyrae variable population, respectively. Hatzidimitriou et al. (1999) concluded that NGC 6426 is coeval with the mean age of the metal-poor Galactic GCs.

4.2. IC 4499

The first CCD photometry of IC 4499 was published by Sarajedini (1993) wherein a $B-V$ CMD extending ∼3 mags below the HB was presented. IC 4499 is exceptional for its prodigious RR Lyrae population. Suntzeff et al. (1991) compiled luminosity-normalized RR Lyrae populations for 77 Galactic GCs.[2] On a scale where $N_{RR} = 0.3$ for 47 Tuc and $N_{RR} = 56.4$ for M 3, the N_{RR} value of IC 4499 is 88.7. The only GC with a higher value of N_{RR} is Palomar 13, but with only four RR Lyrae stars its specific frequency is likely to be influenced by small number statistics.

A comprehensive study of the CMD and RR Lyrae population of IC 4499 was performed by Walker & Nemec (1996), who derived a mean reddening of E(B−V)=0.22 ± 0.02 based on four independent estimates and [Fe/H]= -1.65 ± 0.10 on the Zinn & West (1984) scale. Adopting a reddening and metallicity close to these values, Ferraro et al. (1995) conclude that IC 4499 is younger (by 3-4 Gyr) than most globular clusters at its metallicity.

Kunder et al. (2011) presented an updated study of the RR Lyraes in IC 4499 and found that their period change rates were an order of magnitude larger than predicted by stellar models. Walker et al. (2011) presented multi-band, ground-based photometry of IC 4499. Their CMD reaches ∼ 3 mag below the MSTO from which Walker et al. (2011) estimated an age of 12 ± 1 Gyr.

---

[2] The quantity used by Suntzeff et al. (1991), N_{RR}, is an integrated luminosity-averaged quantity: the number of RR Lyraes a GC would have if the GC itself had $M_V = -7.5$.

4.3. Ruprecht 106

Discovered by Ruprecht on photographic plates as he was searching for open clusters (Alter et al. 1961), Ruprecht 106 existed in relative obscurity until the first CCD photometry by Buonanno et al. (1990) showed that it is metal-poor with a red HB and, thus, was likely to be younger than other GCs with similar metallicities. Subsequent work by Buonanno et al. (1993) corroborated this result.

The metal abundance of Ruprecht 106 has been a source of controversy since the work of Buonanno et al. (1990). The abundance studies performed thus far have fallen into two broad categories, those that find a metal abundance of [Fe/H] ~ -1.9 (Buonanno et al. 1990, 1993; Sarajedini & Layden 1997) based on photometric indicators and those that conclude [Fe/H] ~ -1.6 based on spectroscopy (Da Costa et al. 1992; Francois et al. 1997). Kaluzny et al. (1995) found that Ruprecht 106 and M 3 have similar metallicities based on time series photometry of 12 RR Lyrae variables and, separately, that [Fe/H] ≥ -1.6 based on the relative locations of the RGB bump and the HB.

The discrepancy in metallicity estimates may be due to the unusually low [α/Fe] ratio of Ruprecht 106 compared to other metal-poor Galactic GCs (Pritzl, Venn, & Irwin 2005). Brown et al. (1997) claimed [Fe/H]$=\simeq -1.45$ and [O/Fe] ~ 0 based on high-resolution spectra of 2 red giants. VLT/UVES spectroscopy of 6 red giants indicates $-1.5 <$ [Fe/H] < -1.45 and $-0.1 <$ [α/Fe] $< +0.1$ (P. Francois, 2010, private communication).

4.4. Palomar 15

The earliest CCD photometry of Palomar 15 dates back to the work of Seitzer & Carney (1990) and Harris (1991). CMDs presented in both of these studies extend from the tip of the RGB to about 3 mags below the HB and reveal an HB morphology that is blue-ward of the RR Lyrae instability strip. In addition, both studies conclude that Palomar 15 suffers from a higher-than-expected amount of line-of-sight reddening. Whereas the Burstein & Heiles (1982) reddening maps predict E(B$-$V) ~ 0.1, the CMDs of Seitzer & Carney (1990) and Harris (1991) suggest a reddening closer to E(B$-$V) ~ 0.4, consistent with the reddening maps of Schlegel et al. (1998). Given this value, photometric indicators predict [Fe/H] $\sim$ -1.9. The only spectroscopic value of the metallicity was published by Da Costa & Armandroff (1995), who found [Fe/H]$= -2.00 \pm 0.08$ based on the strength of its Calcium triplet lines.

4.5. NGC 7006

NGC 7006 was recognized early-on as a prime example of the second parameter effect. Sandage & Wildey (1967) noted that that M 13, M 3, and NGC 7006 all have very similar metallicities ([Fe/H] ~ -1.6) but exhibit a range of HB morphologies, with M 13 displaying the bluest HB and NGC 7006 the reddest. Despite its importance in this regard, the deepest published CMD remains that of Buonanno et al. (1991), which extends only $\sim$1 mag below the MSTO. Kraft et al. (1998) estimated [Fe/H]= -1.55 based on high-resolution spectra of 6 stars. Kirby et al. (2008) found similar a similar average value from medium-resolution spectra of 20 stars: [Fe/H]= -1.59 ± 0.03.

4.6. Pyxis

Discovered by Weinberger (1995) while searching the optical sky surveys, the Pyxis globular cluster was confirmed as a GC by Da Costa (1995) and, soon thereafter, by Irwin et al. (1995) and Sarajedini & Geisler (1996). These studies revealed a sparsely populated CMD indicative of an intermediate metallicity GC with a red HB. Sarajedini & Geisler (1996) used the simultaneous reddening and metallicity method of Sarajedini (1994) to derive [Fe/H] = -1.20 ± 0.15 and E(B$-$V) = 0.21 ± 0.03 for Pyxis. Spectroscopy of 6 bright giants in Pyxis by Palma et al. (2000) yields a mean metallicity of [Fe/H] = -1.4 ± 0.1, broadly consistent with the abundance derived by Sarajedini & Geisler (1996).

4.7. Palomar 5

The first CCD-based photometry of Palomar 5 was published by Smith et al. (1986) in the B and V filters. As is typical for the Palomar clusters, the CMD of Palomar 5 is relatively sparse on the RGB and HB. Despite the fact that their CMD clearly delineated the MSTO of Palomar 5, Smith et al. (1986) were unable to determine a reliable age estimate for the cluster using the isochrones of VandenBerg & Bell (1985). Grillmair & Smith (2001) presented a deeper, more precise CMD of Palomar 5 based on HST/WFPC2 observations in the $F555W$ and $F814W$ filters, which they converted to ground-based V, I. The resulting CMD extends over 7 magnitudes below the MSTO and was used by Grillmair & Smith (2001) to study the main sequence luminosity function of Palomar 5. Since the study of Grillmair & Smith (2001), Palomar 5 has been the subject of extensive investigations focused on its tidal tails (Grillmair & Dionatos 2006; Odenkirchen et al. 2009). Spectroscopy of four giant stars in Palomar 5 yields a mean metallicity of [Fe/H] ~ -1.3 (Smith et al. 2002) which

is consistent with the abundance inferred from the CMD (Smith et al. 1986). The reddening of Palomar 5 is thought to be relatively low, as noted by Smith et al. (1986), who quote a value of E$(B-V) = 0.03$. The maps of Schlegel et al. (1998) give a reddening of E$(B-V)$ $= 0.056$ in the direction of Palomar 5.

5. Age determinations from isochrone fitting

Dotter et al. (2010) presented isochrone fits to the photometric catalog of the ACS Survey of Galactic GCs, excluding only those known at the time to possess multiple, distinct stellar populations. The fits were performed with isochrones from Dotter et al. (2008). The procedure employed in the isochrone fits presented in this section follows that of Dotter et al. (2010, Sec. 4.2). The distance, reddening, and chemical composition of the isochrones are initially set to the best available literature values (see Table 2) and these are adjusted only when necessary to achieve the best simultaneous agreement between the models and the CMD on the unevolved main sequence and the base of the red giant branch. Dotter et al. (2010, see their Figures 6 and 7) showed that the distances derived in this manner were consistent with the absolute magnitudes of HB stars derived from RR Lyraes with the 1σ uncertainties and that the derived metallicities were typically within 0.1-0.2 dex of spectroscopically determined values, particularly in the range $-2 \leq$ [Fe/H] ≤ -1.5. The values derived from isochrone fitting for the present sample are compared to the values obtained from the literature at the end of this section.

Once the isochrones were registered in this manner, the age is estimated by selecting the isochrone which most closely matches the shape and position of the subgiant branch. The isochrone fits are performed 'by eye' and the quoted uncertainties reflect the width of the data in the CMD and any mismatch between the data and the slope of the models through this region. As such, these uncertainties are suggestive of goodness-of-fit but lack statistical significance. Chaboyer & Krauss (2002) report that uncertainties in stellar models lead to an error of $\pm 3\%$ in derived ages if a star's properties are known exactly. At an age of 13 Gyr, 3% corresponds to ~ 0.4 Gyr. Adding this value in quadrature with a typical uncertainty of 1 Gyr due to the fit (see Table 3) and ~ 0.5 Gyr for 0.2 dex uncertainty in metallicity (e.g., Dotter et al. 2008) leads to a realistic error budget of ~ 1.2 Gyr.

As can be seen in the figures that follow, age effects are only relevant from ~ 2 magnitudes below to ~ 1 magnitude above the MSTO: greater depth in the CMD provides a tighter constraint on the models. The CMDs of Ruprecht 106, IC 4499, and NGC 7006 provide excellent constraints; differential reddening is a limiting factor in NGC 6426, Palomar 15, and Pyxis. The sparseness of the Pyxis and Palomar 15 CMDs also reduces the

precision of the isochrone fitting.

Stars brighter than the subgiant branch are saturated in the WFPC2 observations of Palomar 5. To enable a more robust age determination, the WFPC2 data have been supplemented with ground-based observations from Stetson (2000). For the ∼20 stars that appear in both catalogs, the average offsets are less than 0.01 mag in V and I; the WFPC2 data were adjusted to match the photometric zeropoints of the standard stars measured by Stetson (2000).

The isochrone fits are shown in Figures 7, 8, and 9; the results of isochrone fitting are presented in Table 3. For comparison purposes, the reddening and distance values listed in Table 3 have been transformed to standard $\mathrm{DM_V}$ and $E(B-V)$ using the extinction coefficients given by Sirianni et al. (2005). The CMDs in Figures 7 and 8 were cleaned to improve the clarity of the fits by selecting stars according to photometric errors and other diagnostic information as described by Anderson et al. (2008, Section 7). As check on the results of isochrone fitting, synthetic zero age HB model sequences for the color ranges appropriate for each GC are plotted in Figures 7-9 as dashed lines. Generally speaking, these comparisons lend confidence to the results of the isochrone fitting. However, note that the models appear to inadequately represent those GCs that harbor both red and blue HB stars and, further, that the scarcity of HB stars in Pyxis and Palomar 5 make these comparisons of relatively little use.

Comparison of the [Fe/H] values listed in Tables 2 and 3 indicate that the literature values and those adopted in the isochrone fits differ, at most, by 0.1 dex in [Fe/H]. The largest departures are in cases where no information regarding [α/Fe] is available. Comparison of the derived distance moduli shows that 4 of 7 GCs considered here differ by less than 0.05 mag. The largest discrepancy in distance modulus, that of Ruprecht 106, also corresponds to the largest discrepancy in [Fe/H] between the Harris (1996) catalog and the adopted spectroscopic value. The Harris catalog distances are based a the relation between the absolute magnitude of the RR Lyrae stars and the mean [Fe/H] of the GC.

6. The age-metallicity relation of Galactic globular clusters

As described in §2, all aspects of the observations and data reduction of the 6 GCs observed with ACS in program GO-11586 were designed to be homogeneous with the ACS Survey of Galactic GCs. The observations and data reductions of Palomar 5 are consistent with the outer halo GCs studied by Stetson et al. (1999) and Dotter et al. (2008). The isochrone analysis of all 7 GCs presented herein is consistent with the approach used in

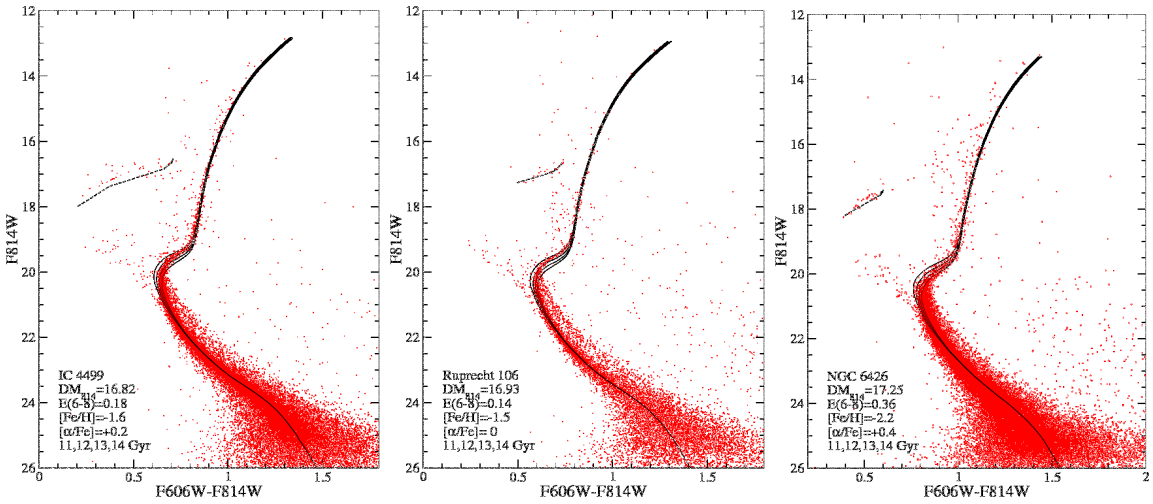

Fig. 7.— GCs at 15-20kpc.

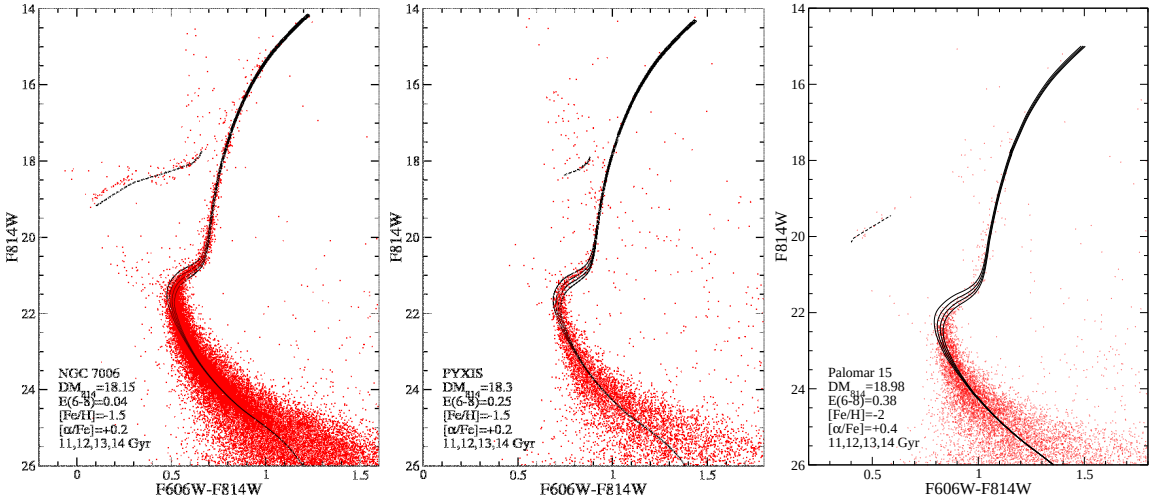

Fig. 8.— GCs at $\sim$ 40kpc.

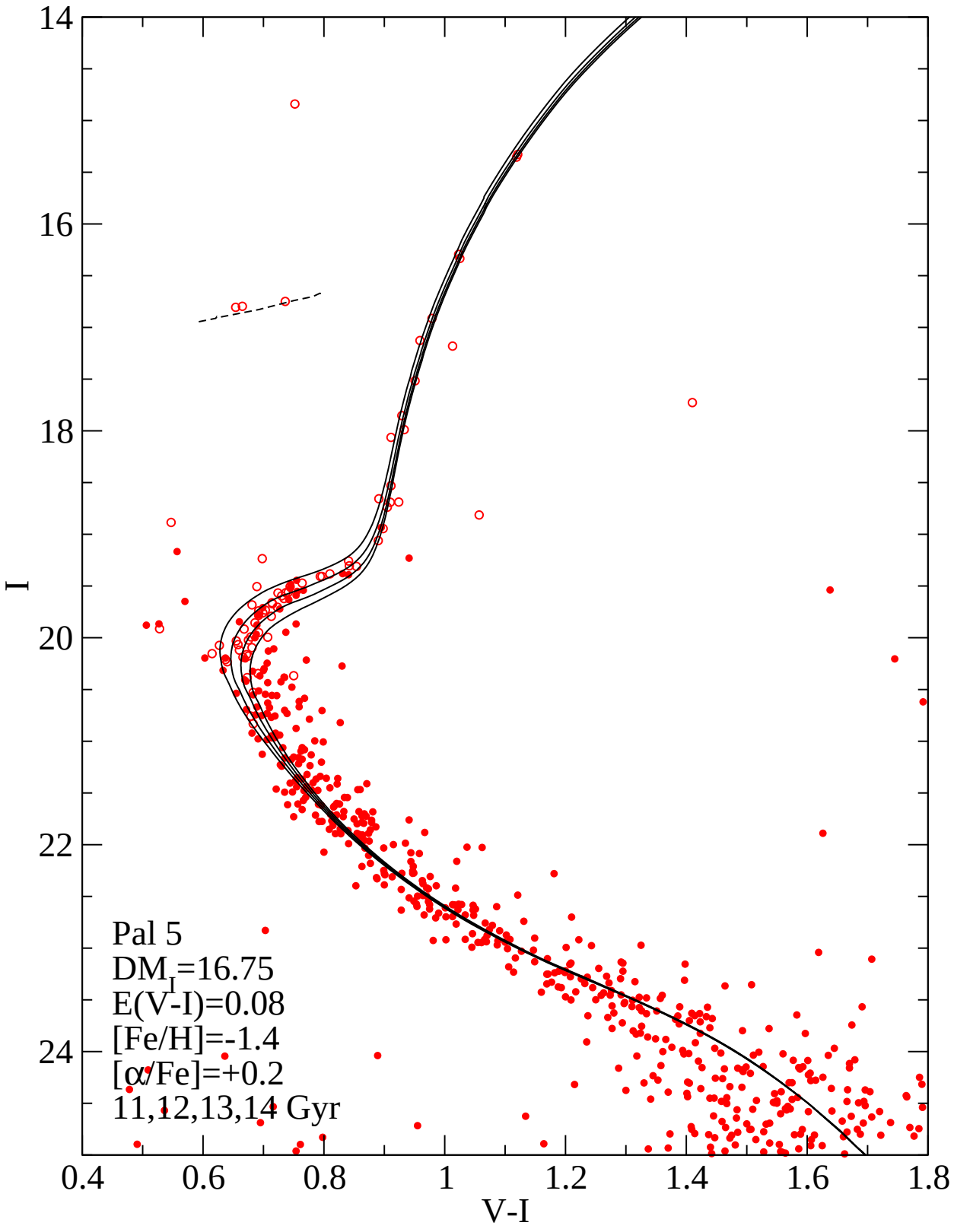

Fig. 9.— Isochrone fits to the HST/WFPC2 CMD of Palomar 5 in the ground V, I system. The WFPC2 data are shown as filled circles and the ground-based data as open circles.

Dotter et al. (2008) and Dotter et al. (2010). Hence, the results in Table 3 can be incorporated into the AMR assembled by Dotter et al. (2010).

The upper-left panel of Figure 10 shows the AMR of Dotter et al. (2010) with filled circles indicating $R_{GC} \leq 8$ kpc and diamonds indicating $R_{GC} > 8$ kpc. The current sample are plotted as open diamonds to highlight where they fall on the AMR. In order to give a sense of the uncertainties in the diagram, a 'typical' error bar representing ± 0.2 dex in [Fe/H] and ± 1 Gyr in age is plotted in every panel of Figure 10. The remaining panels compare the GC AMR to various model predictions: the upper-right panel shows the simple closed-box chemical evolution model for the Sagittarius dwarf spheroidal galaxy from Siegel et al. (2007); the lower-left panel shows the chemical evolution models of the Magellanic Clouds from Pagel & Tautvaišienė (1998); and the lower-right panel shows the mean trend from the GC formation model of Muratov & Gnedin (2010). These comparisons are discussed in the following paragraphs.

The closed-box model portrayed in the upper-right panel of Figure 10 was taken from the study of the star formation history of M 54 and the central field of the Sagittarius (hereafter Sgr) dwarf spheroidal galaxy by Siegel et al. (2007). The star formation history was derived with the same stellar models used in this paper and photometry from the ACS Survey of Galactic GCs. It has already been demonstrated by Layden & Sarajedini (2000) that the GCs associated with Sgr follow the same trend as its field stars. Forbes & Bridges (2010) reiterate that the AMR of Sgr is essentially identical to that of the putative Canis Major (CMa) dwarf galaxy and argue that ~ 20 GCs originated with one or the other. The upper-right panel of Figure 10 indicates that the outer halo GCs follow an AMR consistent with dwarf galaxy chemical evolution. However, it appears that the outer halo GCs formed in a variety of environments within which chemical enrichment proceeded at different rates; one characteristic of Sgr or CMa is insufficient to explain the observed AMR.

The GC AMR is compared to the AMRs of the Small and Large Magellanic Cloud (SMC and LMC) chemical evolution models by Pagel & Tautvaišienė (1998) in the lower-left panel of Figure 10. The LMC AMR is not markedly different from that of M 54/Sgr, as pointed out by Forbes & Bridges (2010). The SMC AMR tracks the majority of GCs with ages less than 12 Gyr better than either the LMC or M 54/Sgr.

The comparisons with Sgr and the MCs indicate that a collection of dwarf galaxies with a range of AMRs are likely to have contributed to the Galactic GC population, consistent with the findings of Forbes & Bridges (2010). Muratov & Gnedin (2010) devised a semi-analytical model of the formation of a massive host galaxy's GC population and trained their model on the Galactic GC metallicity distribution. The model is built on top of cold dark matter galaxy formation simulations and assigns a globular cluster formation probability and

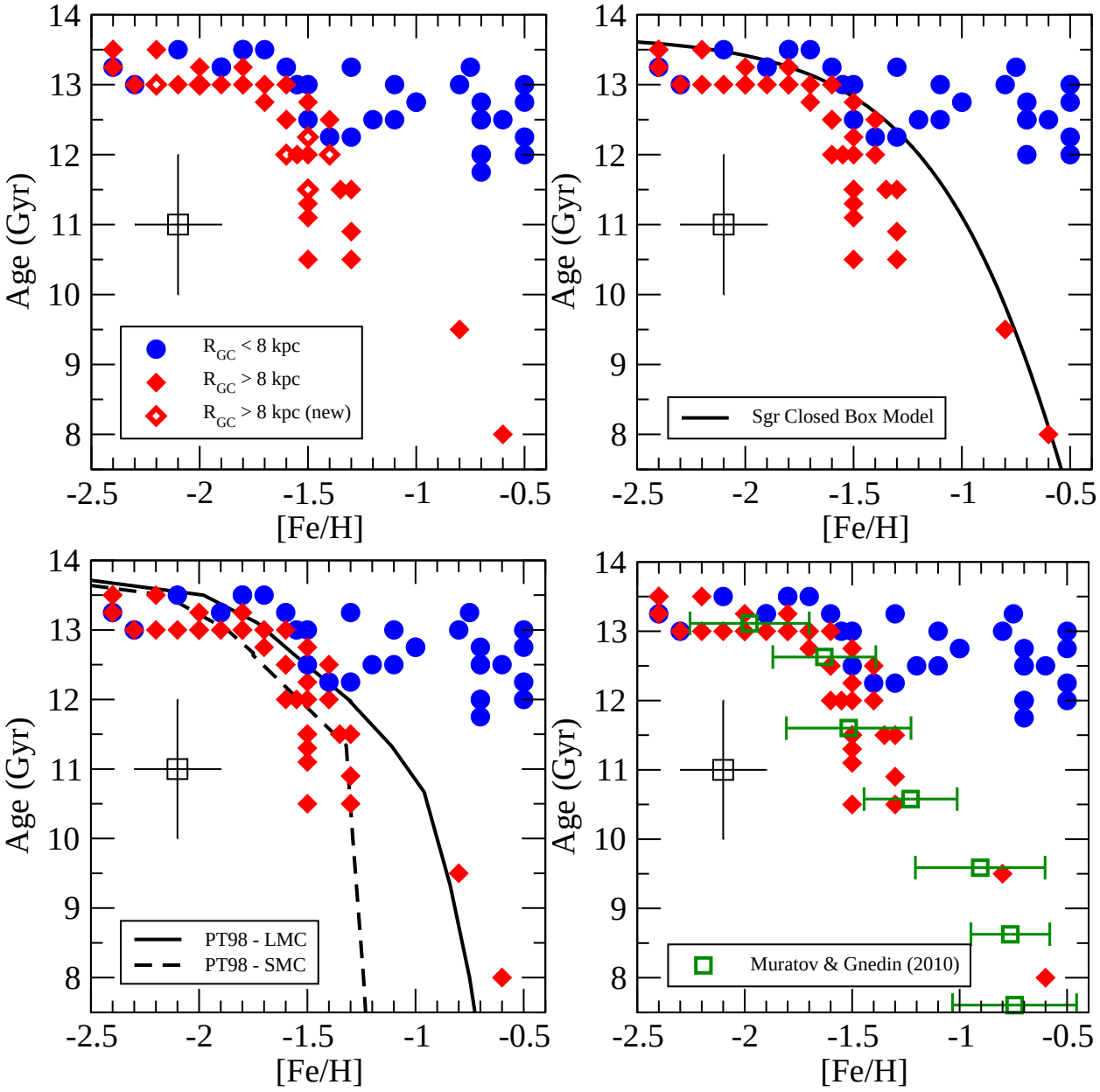

Fig. 10.— *Upper left:* The AMR from Dotter et al. (2010) with points identifying individual GCs by $R_{GC} \leq 8$ kpc (filled circles) and $R_{GC} > 8$ kpc (filled diamonds). The current sample are shown as open diamonds. *Upper right:* The AMR with the M 54/Sagittarius closed box model. *Lower left:* The AMR with the LMC and SMC models from Pagel & Tautvaišienė (1998). *Lower right:* The AMR with the mean trend from the Muratov & Gnedin (2010) models. The GC symbols are the same as in the upper-left panel except that the current sample is not highlighted. See text for discussion.

chemical enrichment history to each sub-halo that is accreted by the host galaxy. Among their stated goals is the development of a bimodal color distribution in the GC population without requiring two distinct formation mechanisms. While the model achieves this goal by design, it also fits the age-metallicity distribution of the outer halo GCs remarkably well. The lower-right panel of Figure 10 compares the GC AMR with the mean trend (squares) and standard deviation (indicated by error bars) of [Fe/H] for 0.5 Gyr age bins of nearly 10,000 simulated GCs drawn from the Muratov & Gnedin (2010) model. While the outer halo GCs are well represented by the mean trend, the model is discrepant with the metal-rich GCs in the inner Galaxy, i.e., the bulge and thick disk GCs. Muratov & Gnedin attribute this discrepancy to the lack of a metallicity gradient within the individual merging halos. As a substantial fraction of the Galactic GC population is old and metal-rich, it behooves a model of the GC population formation to describe the origins of these GCs.

7. Discussion

The AMRs constructed by Marín-Franch et al. (2009) and Dotter et al. (2010, further updated in this paper) show that Galactic GCs split into two distinct branches at [Fe/H] $\gtrsim -1.5$. Marín-Franch et al. (2009) interpreted this branching as representing two groups of GCs: an old group with uniformly old ages (a flat AMR) and a young group with a significant trend toward younger ages at higher metallicities. They concluded that these groups likely originated from two different phases of Galaxy formation: an initial, relatively brief collapse and a second, prolonged episode driven by accretion. Marín-Franch et al. (2009) found a small number of metal-poor ([M/H] ≤ -1.5) GCs with somewhat younger ages than the bulk of the metal-poor GCs. Dotter et al. (2010) and the present study find all of the metal-poor GCs to be uniformly old,[3] but this difference does not substantially influence the conclusion with respect to the proposed Galaxy formation scenario.

A number of influential studies have used the HB morphology-metallicity diagram to infer the ages of stellar populations for which metallicity information and good photometry to at least the level of the HB are available. For example, Catelan & de Freitas Pacheco (1993) and Lee, Demarque, & Zinn (1994) both used synthetic HB models to demonstrate that, under the assumption of constant mass loss, the Galactic GC HB morphology-metallicity diagram showed evidence for an age spread of several (~ 4) Gyr for a fixed He content and heavy element distribution.

The use of the HB morphology-metallicity diagram must, however, remain a crude age

[3]See Figure 9 of Dotter et al. (2010) for a direct comparison of the AMRs.

indicator at best for a variety of reasons. The lack of detailed abundance information, including the possible spread in He within a given GC, has important implications for HB morphology. The effect of a spread in the total He content on HB morphology *among* different GCs has been explored by many authors (see, e.g., Catelan & de Freitas Pacheco 1993; Lee, Demarque, & Zinn 1994) as well as a spread in He *within* single GCs (see, e.g., D'Antona & Caloi 2008). Another important factor in matching GC HB morphology to model predictions is statistical fluctuations. The ACS GC Treasury project photometric database contains GCs with anywhere from ~ 20 to several hundred HB stars, leading to uncertainty in the median color of the HB of up to 30% in the sparsest GC (Dotter et al. 2010, Table 1).

Addressing the question of which parameters most strongly influence HB morphology using full CMDs for large samples of GCs, Dotter et al. (2010) and Gratton et al. (2010) reached the same conclusion: that age is the second parameter influencing HB morphology. The results presented in this paper lend further support to this conclusion. It is important to note that the term 'second parameter' used here applies specifically to the variation of HB morphology *among* different GCs, the context in which the term was originally used in the 1960's (e.g., van den Bergh 1967; Sandage & Wildey 1967). 'Second parameter' is not intended to apply to the spread in HB stars within a single GC, for which the same term is often employed, nor does this paper seek to address that important issue. Dotter et al. (2010) and Gratton et al. (2010) both found evidence for at least a third parameter as well, suggesting that age and metallicity alone are not sufficient to fully characterize HB morphology.

Figure 11 shows the HB morphology-metallicity diagram of the full sample of 68 GCs. The left panel considers HB morphology as the median color difference between the HB and RGB (Dotter et al. 2010) and the right panel instead uses the (B−R)/(B+V+R) metric of Lee (1989) as compiled by Mackey & van den Bergh (2005). Dotter et al. (2010) demonstrated that these two HB morphology metrics are strongly correlated, with the main difference being that $\Delta(V-I)$ does not saturate as (B−R)/(B+V+R) does at ± 1. In this context, it is clear that age is the second parameter influencing HB morphology as concluded by Dotter et al. (2010) and Gratton et al. (2010).

While Figure 11 is not well sampled over the full range of metallicity, it can still be seen that the transition from a red HB to a blue one happens over $\lesssim 0.5$ dex in [Fe/H] for a fixed age, or $\lesssim 2$ Gyr at fixed [Fe/H]. It is interesting to consider the ensemble in this manner, despite the fact that age uncertainties remain at or near the 10% level. It is a fortunate coincidence that we observe these GCs at a time when the HB morphology-metallicity diagram is rich with information. Turn the clock back ~ 2 Gyr and the HB

Table 3. Results of isochrone fitting

Cluster	DM_V	$E(B-V)$	[Fe/H]	[α/Fe]	Age (Gyr)
IC 4499	17.07	0.18	−1.6	0.2	12.0 ± 0.75
Ruprecht 106	17.12	0.14	−1.5	0.0	11.5 ± 0.5
NGC 6426	17.74	0.36	−2.2	0.4	13.0 ± 1.5
NGC 7006	18.16	0.04	−1.5	0.2	12.25 ± 0.75
Pyxis	18.64	0.25	−1.5	0.2	11.5 ± 1.0
Palomar 15	19.50	0.38	−2.0	0.4	13.0 ± 1.5
Palomar 5	16.86	0.08	−1.4	0.2	12.0 ± 1.0

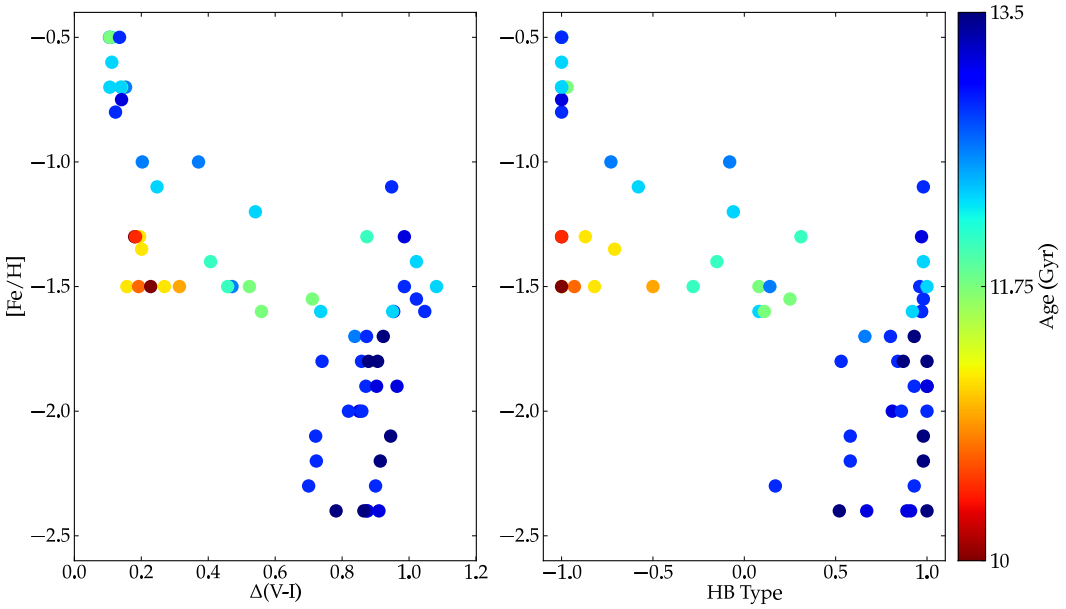

Fig. 11.— A demonstration of the age effect in the HB morphology-metallicity diagram using ages derived from the MSTO. The left panel shows the Δ(V − I) metric as compiled by Dotter et al. (2010) and this study; the right panel shows (B−R)/(B+V+R) as compiled by Mackey & van den Bergh (2005). The shade of each point corresponds to its age with the oldest GCs shown as blue and the youngest shown as red.

morphology-metallicity diagram would have been populated only on the red side—as, for example, in the SMC (Glatt et al. 2008). At such a time, the study by Searle & Zinn (1978) would have revealed little variation in HB morphology among the halo GCs and, hence, little or no insight into the formation of the Galaxy. Only the truly peculiar GCs, such as NGC 2808 (Dalessandro et al. 2010), might have shown a sizable variation. On the other hand, turn the clock forward ~ 2 Gyr and all but the most metal-rich Galactic GCs would have blue HBs.

8. Summary

HST/ACS photometry of 6 Galactic halo GCs, IC 4499, NGC 6426, NGC 7006, Palomar 15, Pyxis, and Ruprecht 106, were presented. The resulting CMDs were used to derive ages via isochrone fitting. The age of Palomar 5 was derived using the same set of models and the combined photometry of Grillmair & Smith (2001) and Stetson (2000). The ages and metallicities of these 7 GCs were added to the AMR of Dotter et al. (2010). The total number of homogeneously studied GCs in the sample is 68, excluding those 7 GCs imaged by the ACS Survey of Galactic GCs that are known to harbor multiple, distinct stellar populations. Divided at $R_{GC} = 8$ kpc, the inner Galaxy GCs exhibit a pattern of rapid chemical enrichment spanning two orders of magnitude in metallicity over a timescale of 1-2 Gyr. The outer Galaxy GCs exhibit a much slower chemical enrichment that is evocative of dwarf galaxy chemical evolution and is reasonably well matched by the semi-analytic GC formation models of Muratov & Gnedin (2010).

Data presented in this paper were obtained from the Multimission Archive at the Space Telescope Science Institute (MAST). Support for this work (proposal GO-11586) was provided by NASA through a grant from the Space Telescope Science Institute, which is operated by the Association of Universities for Research in Astronomy, Inc., under NASA contract NAS5-26555. This research has made use of NASA's Astrophysics Data System Bibliographic Service as well as the SIMBAD database, operated at CDS, Strasbourg, France.

REFERENCES

Alter, G., Hogg, H. S., Ruprecht, F., & Vanýsek, V. 1961, BAICz, 12

Anderson, J. & Bedin, L. R. 2010, PASP, 122, 1035

Anderson, J., et al. 2008, AJ, 135, 2055

Bedin, L. R., Cassisi, S., Castelli, F., Piotto, G., Anderson, J., Salaris, M., Momany, Y., Pietrinferni, A. 2005, MNRAS, 357, 1038

Bohlin, R. C. 2007, Instrument Science Report ACS 2007-06

Brown, J. A., Wallerstein, G., & Zucker, D. 1997, AJ, 114, 180

Buonanno, R., Buscema, G., Fusi Pecci, F., Richer, H. B., & Fahlman, G. G. 1990, AJ, 100, 1811

Buonanno, R., Corsi, C. E., Fusi Pecci, F., Richer, H. B., & Fahlman, G. G. 1993, AJ, 105, 184

Buonanno, R., Fusi Pecci, F., Capellaro, E., Ortolani, S., Richtler, T., & Geyer, E. H. 1991, AJ, 102, 1005

Burstein, D. & Heiles, C. 1982, AJ, 87, 1165

Catelan, M & de Freitas Pacheco, J. A. 1993, AJ, 106, 1858

Chaboyer, B., Demarque, P., & Sarajedini, A. 1996, ApJ, 459, 558

Chaboyer, B. & Krauss, L. M. 2002, ApJ, 567, 45

Chaboyer, B., Sarajedini, A., & Demarque, P. 1992, ApJ, 394, 515

Da Costa, G. S. 1995, PASP, 107, 937

Da Costa, G. S. & Armandroff, T. E. 1995, AJ, 109, 2533

Da Costa, G. S., Armandroff, T. E., & Norris, J. E. 1992, AJ, 104, 154

Dalessandro, E., Salaris, M., Ferraro, F. R., Cassisi, S., Lanzoni, B., Rood, R. T., Fusi Pecci, F., & Sabbi, E. 2010, MNRAS, 410, 694

D'Antona, F. & Caloi, V. 2008, MNRAS, 390, 693

Dotter, A., et al. 2010, ApJ, 708, 698

Dotter, A., Sarajedini, A., & Yang, S.-C. 2008, AJ, 136, 1407

Ferraro, I., Ferraro, F. R., Fusi Pecci, F., Corsi, C. E., & Buonanno, R. 1995, MNRAS, 275, 1057

Font, A. S., Johnston, K. V., Bullock, J. S., & Robertson, B. E. 2006, ApJ, 638, 585

Forbes, D. A., & Bridges, T. 2010, MNRAS, 404, 1203

Francois, P., Danziger, J., Buonanno, R., & Perrin, M. N. 1997, A&A, 327, 121

Glatt, K. et al. 2008, AJ, 136, 1703

Gratton, R. 1985, A&A, 147, 169

Gratton, R. G., Carretta, E., Bragaglia, A., Lucatello, S., & D'Orazi, V. 2010, A&A, 517, 81

Grillmair, C. J. & Dionatos, O. 2006, ApJ, 641, L37

Grillmair, C. J. & Smith, G. H. 2001, AJ, 122, 3231

Harris, W. E. 1991, AJ, 102, 1348

Harris, W. E. 1996, AJ, 112, 1487

Harris, W. E., Bell, R. A., Vandenberg, D. A., Bolte, M., Stetson, P. B., Hesser, J. E., van den Bergh, S., Bond, H. E., Fahlman, G. G., & Richer, H. B. 1997, AJ, 114, 1030

Hatzidimitrio, D., Papadakis, I., Croke, B. F. W., Papamastorakis, I., Paleologou, E. V., Xanthopoulos, E. & Haerendel, G. 1999, AJ, 117, 3059

Irwin, M. J., Demers, S., & Kunkel, W. E. 1995, ApJ, 453, 21

Kaluzny, J., Krzeminski, W., Mazur, B. 1995, AJ, 110, 2206

Kirby, E. N., Guhathakurta, P., & Sneden, C. 2008, ApJ, 682, 1217

Koch, A. & Côté, P. 2010, A&A, 517, 59

Koch, A., Côté, P., & McWilliam, A. 2009, A&A, 506, 729

Kraft, R. P., Sneden, C., Smith, G. H., Shetrone, M. D., & Fulbright, J. 1998, AJ, 115, 1500

Kunder, A. et al. 2011, AJ, 141, 15

Larson, R. B. 1972, Nature, 236, 21

Layden, A. C. & Sarajedini, A. 2000, AJ, 119, 1760

Lee, Y.-W. 1989, Ph.D. Thesis, Yale University, New Haven, CT.

Lee, Y.-W., Demarque, P., & Zinn, R. 1994, ApJ, 423, 248

Mackey, A. D. & van den Bergh, S. 2005, MNRAS, 360, 631

Marín-Franch, A., et al. 2009, ApJ, 694, 1498

Muratov, A. L. & Gnedin, O. Y. 2010, ApJ, 718, 1266

Odenkirchen, M., Grebel, E. K., Kayser, A., Rix, H. -W., & Dehnen, W. 2009, AJ, 137, 3378

Pagel, B. E. J. & Tautvaišienė, G. 1998, MNRAS, 299, 535

Palma, C., Kunkel, W. E., & Majewski, S. R. 2000, PASP, 112, 1305

Papadakis, I., Hatzidimitrio, D., Croke, B. F. W., & Papamastorakis, I. 2000, AJ, 119, 851

Piotto, G., et al. 2002, A&A, 391, 945

Pritzl, P. J., Venn, K. A., & Irwin, M. 2005, AJ, 130, 2140

Robertson, B., Bullock, J. S., Font, A. S., Johnston, K. V., Hernquist, L. 2005, ApJ, 632, 872

Sandage, A. & Wildey, R. 1967, ApJ, 150, 469

Sarajedini, A. 1993, AJ, 105, 2172

Sarajedini, A. 1994, AJ, 107, 618

Sarajedini, A., et al. 2007, AJ, 133, 1658

Sarajedini, A. & Geisler, D. 1996, AJ, 112, 2013

Sarajedini, A. & King, C. R. 1989, AJ, 98, 1624

Sarajedini, A. & Layden, A. 1997, AJ, 113, 264

Sarajedini, A., Lee, Y. W., & Lee, D. H. 1995, ApJ, 450, 712

Schlegel, D. J., Finkbeiner, D. P., & Davis, M. 1998, ApJ, 500, 525

Searle, L. & Zinn, R. 1978, ApJ, 225, 357

Seitzer, P. & Carney, B. W. 1990, AJ, 99, 229

Siegel, M. H. et al. 2007, ApJ, 667, 57

Sirianni, M. et al. 2005, PASP, 117, 1049

Smith, G. H., McClure, R. D., Stetson, P. B., Hesser, J. E., & Bell, R. A. 1986, AJ, 91, 842

Smith, G. H., Sneden, C., & Kraft, R. P. 2002, AJ, 123, 1502

Stetson, P. B. 2000, PASP, 112, 925

Stetson, P. B., Bolte, M., Harris, W. E., Hesser, J. E., van den Bergh, S., Vandenberg, D. A., Bell, R. A., Johnson, J. A., Bond, H. E., Fullton, L. E., Fahlman, G. G., & Richer, H. B. 1999, AJ, 117, 247 (S99)

Suntzeff, N. B., Kinsman, T. D., & Kraft, R. P. 1991, ApJ, 367, 528

Tinsley, B. M. & Larson, R. B. 1978, ApJ, 221, 554

VandenBerg, D. A. & Bell, R. A. 1985, ApJS, 58, 561

van den Bergh, S. 1965, JRASC, 59, 151

Walker, A. R. et al. 2011, MNRAS in press (http://arxiv.org/abs/1103.4144)

Walker, A. R. & Nemec, J. M. 1997, AJ, 112, 2026

Weinberger, R. 1995, PASP, 107, 58

Zentner, A. R. & Bullock, J. S. 2003, ApJ, 598, 49

Zinn, R. & Barnes, S. 1996, AJ, 112, 1054

Zinn, R. & West, M. J. 1984, ApJS, 55, 45 (ZW84)